One-Pot Synthesis of Highly Emissive Dipyridinium Dihydrohelicenes

Amedeo Santoro*[a], Rianne M. Lord[a], Jonathan J. Loughrey[a], Patrick C. McGowan[a], Malcolm A. Halcrow*[a], Adam F. Henwood[b], Connor Thomson[b] and Eli Zysman-Colman*[b]

Abstract: Condensation of a pyridyl-2-carbaldehyde derivative with 2-(bromoethyl)amine hydrobromide affords tetracyclic pyrido[1,2-*a*]pyrido[1',2':3,4]imidazo-[2,1-*c*]-6,7-dihydropyrazinium dications in excellent yields. Crystal structures and NOE data demonstrate the helical character of the dications, the dihedral angles between the two pyrido groups ranging from 28-45°. An intermediate in the synthesis was also characterized. A much brighter emission compared to literature helicenes has been found, with quantum yields as high as 60% in the range of 460-600 nm. Preliminary cytotoxicity studies against HT-29 cancer cells demonstrated moderate-to-good activity, with IC_{50} values 12-30x that of cisplatin.

Helical poly-aromatic compounds (helicenes) are of intense current interest.[1-3] Apart from the synthetic challenges involved in preparing and resolving such compounds,[1,2,4] they are useful auxiliary groups for asymmetric reactions and chiral catalysis.[3,5] Helicenes and their derivatives can be chiral components in self-assembly systems[1,3,6] and macromolecular materials,[3,7] while many helicenes are fluorescent, with a chiral emission when optically pure. Moreover, helicenes containing quinone,[4] pyridinium[8–10] or thieno[11] fragments, or an appended metal ion,[12] are redox-active and therefore switchable. This has led to the development of organic light-emitting diodes (OLEDs) and other chiroptical devices based on helicene fluorophores.[3,13]

The synthesis of pyrido[1,2-*a*]pyrido[1',2':3,4]imidazo-[2,1-*c*]-6,7-dihydropyrazinium dibromide (**1Br$_2$**, Scheme 1) by an acid-catalysed reaction of pyridine-2-carboxaldehyde with (2-bromoethyl)amine was first reported by Glover *et al.* in 1969.[14] They proposed a mechanism for the transformation,[15] and described the reactivity of **1Br$_2$** towards basic hydrolysis and hydrogenation. We fortuitously prepared **1Br$_2$** during our studies of heterocyclic chelate ligands for transition ions,[16] and report now a more detailed study of this [4]-helical heterocycle and its derivatives. While no more detailed structural or physical data from **1Br$_2$** have been reported so far, we note its relationship to diquat helicene derivatives,[8–10] some of which exhibit particularly favorable chiroptical properties.[9]

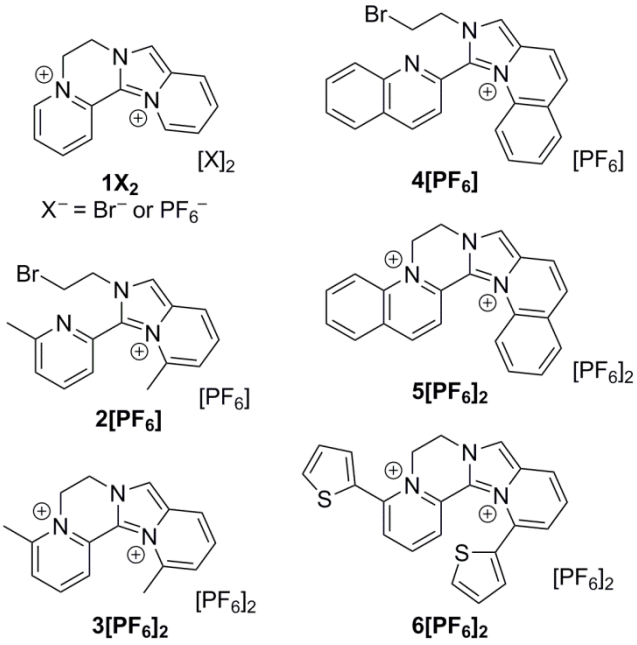

Scheme 1. Compounds referred to in this work.

As previously described,[14] reaction of pyridine-2-carboxaldehyde with (2-bromoethyl)amine hydrobromide in equimolar ratios in THF at room temperature affords **1Br$_2$** as a brown precipitate in good yield. The freshly prepared precipitate is analytically pure, but can be recrystallized from ethanol/water to afford monohydrate crystals **1Br$_2$**·H_2O. Treatment of aqueous **1Br$_2$** with excess NH_4PF_6 precipitates **1[PF$_6$]$_2$**, which is more soluble in organic solvents. Repeating the procedure using 6-methylpyridine-2-carboxaldehyde, quinoline-2-carboxaldehyde or 6-(2-thienyl)-pyridine-2-carboxaldehyde afforded the disubstituted derivatives **3[PF$_6$]$_2$**, **5[PF$_6$]$_2$** and **6[PF$_6$]$_2$** respectively. More forcing conditions were needed to push these reactions to completion, however, and the 2-(2-bromoethyl)-3-(pyridin-2-yl)imidazo-[1,5-*a*]-pyridinium intermediates **2[PF$_6$]** and **4[PF$_6$]** were also isolated from such reactions performed at room temperature. While **2[PF$_6$]** was obtained as a pure solid, **4[PF$_6$]** was always contaminated with **5[PF$_6$]$_2$** and was purified for characterization by a Pasteur separation. Hence, a wider physicochemical study of that compound was not undertaken. Heating **2[PF$_6$]** and **4[PF$_6$]** in DMF at 100 °C caused their stoichiometric conversion to **3[PF$_6$]$_2$** and **5[PF$_6$]$_2$** by ^{1}H NMR.[15]

Single crystal *X*-ray structure determinations of **1Br$_2$**·H_2O; **3[PF$_6$]$_2$**, **4[PF$_6$]**, **5[PF$_6$]$_2$** and **6[PF$_6$]$_2$**·CH_3OH confirmed their respective connectivity (Fig. 1). The metric parameters within the tetracyclic framework are consistent with the tautomeric

[a] Dr. A. Santoro, Dr. R. M. Lord, Dr. J. J. Loughrey, Dr. P. C. McGowan, Prof. M. A. Halcrow
School of Chemistry, University of Leeds, Woodhouse Lane, Leeds, LS2 9JT, UK.
E-mail: a.santoro@leeds.ac.uk; m.a.halcrow@leeds.ac.uk
[b] A. F. Henwood, C. Thomson, Dr. E. Zysman-Colman
EaStCHEM School of Chemistry, University of St Andrews, St Andrews, Fife, KY16 9ST, UK.
E-mail: eli.zysman-colman@st-andrews.ac.uk

Supporting information for this article is given via a link at the end of the document.

structures shown, with clear single/double bond length alternation in the imidazo[1,5-*a*]pyridinium fragments.[17] The tetracyclic dications all adopt helical conformations with the degree of helicity, as measured by the dihedral angle between the two pyrido rings (ω), being:

$$\mathbf{1}^{2+}\ [\omega = 27.64(6)°] < \mathbf{3}^{2+}\ [36.39(4)°] \approx \mathbf{6}^{2+}\ [37.19(8)°] < \mathbf{5}^{2+}\ [45.23(4)°]$$

This non-planarity reflects an intramolecular contact between the H atoms bound to pyridinium *C*3 and imidazo[1,5-*a*]pyridinium *C*5 (C(5) and C(14) in Fig. 1), which are 2.19 Å apart in **1Br$_2$**·H$_2$O.[18] This steric repulsion is exacerbated in $\mathbf{3}^{2+}$, $\mathbf{5}^{2+}$ and $\mathbf{6}^{2+}$, which have substituents at the imidazo[1,5-*a*]pyridinium *C*5 position. Only **3[PF$_6$]$_2$** crystallizes as optically pure helical molecular crystals, in a chiral space group. The crystal examined has *P* (Δ) helicity, but equal numbers of *P*- and *M*-helical crystals are present in the bulk sample. The other three dications form racemate crystals, in centrosymmetric space groups. Most of the helicity is generated by rotation about the C(6)−C(7) bond in the dihydropyrazinium ring (Fig. 1), although a sterically-induced bending of the conjugated imidazo[1,5-*a*]pyridinium fragment is also evident, particularly in **3[PF$_6$]$_2$**. The conformational strain implied by this increased helicity accounts for our isolation of **2[PF$_6$]** and **4[PF$_6$]**, and the need for forcing conditions to complete the synthesis of **3[PF$_6$]$_2$** and **5[PF$_6$]$_2$**. Consistent with that, the quinolyl and imidazo[1,5-*a*]quinolinium groups in **4[PF$_6$]** are close to perpendicular [ω = 78.27(3)°], reflecting the relief of steric congestion between these groups by free rotation about the C(5)−C(6) bond.[17] The retention of these helical conformations in CD_3CN solution was confirmed by NOESY analyses, which demonstrated strong NOE enhancements between the pyridinium *H*3 atom and either the imidazo[1,5-*a*]pyridinium *H*5 atom (**1[PF$_6$]$_2$**), or the methyl group at that position (**3[PF$_6$]$_2$**).[17]

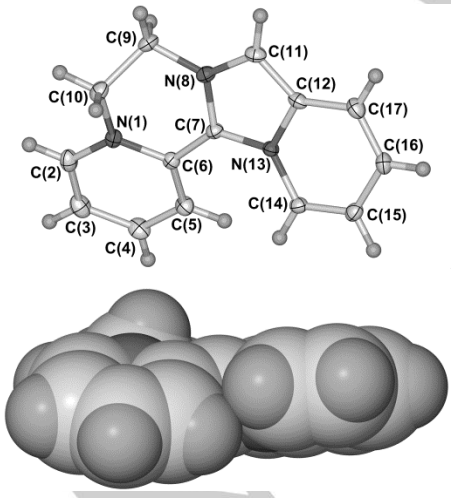

Figure 1. Top: view of the $\mathbf{1}^{2+}$ dication in the crystal structure of **1Br$_2$**·H$_2$O. Thermal displacement ellipsoids are set at 50 %. Bottom: space-filling view of $\mathbf{1}^{2+}$, showing the intramolecular steric clash that gives rise to the helicity. The view is along the C(7)–N(8) bond.[17]

Polyaromatic dyes can be DNA intercalators, which bind between stacked base pairs in the DNA double helix.[19] Since DNA intercalators can inhibit nucleic acid synthesis *in vivo* and are therefore cytotoxic,[20] a preliminary cytotoxicity study was performed by screening **1Br$_2$**·H$_2$O, **1[PF$_6$]$_2$**, **2[PF$_6$]** and **5[PF$_6$]$_2$** against HT-29 (human colon adenocarcinoma) cancer cells. The salts **1Br$_2$** and **1[PF$_6$]$_2$** exhibit moderate cytotoxicities against this cell line, compared to a cisplatin standard measured under the same conditions (Table 1). Their identical IC_{50} values imply that the counterions Br^- and PF_6^- have no influence on cell viability. The other two compounds show improved IC_{50} values, of *ca.* 10x higher than cisplatin. This might be attributed to different factors in the two compounds. First is the conformational flexibility of $\mathbf{2}^+$, whose pyridinium and imidazo-[1,5-*a*]pyridinium groups can rotate freely with respect to each other. That will allow $\mathbf{2}^+$ to adjust its conformation in response to the steric environment about the DNA nucleobase stacks. Second, is the extended conjugation of the quinolinium groups in **5[PF$_6$]$_2$**, which increases its hydrophobicity and promotes strong intercalative π–π interactions with the DNA bases.

Table 1. Cytotoxicity data for compounds in this work, and a cisplatin standard, against the HT-29 cancer cell line.

Compound	IC_{50} (μM)	Compound	IC_{50} (μM)
1Br$_2$·H$_2$O	107±3	**2[PF$_6$]**	64±1
1[PF$_6$]$_2$	110±2	**5[PF$_6$]$_2$**	44±1
		Cisplatin	3.6±0.2

Aside from their biological activity, these compounds also demonstrate interesting photophysical and electrochemical properties (Table 2, Fig. 2).[8,10] Assignment of their UV/vis absorption bands is hindered by limited literature precedent.[8,9] However, based on their energies, we have tentatively ascribed the high energy bands (270-350 nm) of these compounds as typical π–π* localized transitions, while the lower energy bands are plausibly charge transfer (CT) transitions between the charged pyridinium and imidazolium rings.

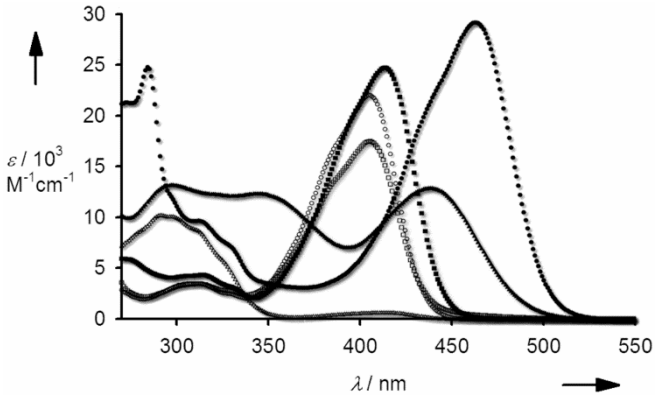

Figure 2. UV/vis spectra of **1Br$_2$** (□), **1[PF$_6$]$_2$** (○), **2[PF$_6$]** (△), **3[PF$_6$]$_2$** (■), **5[PF$_6$]$_2$** (●) and **6[PF$_6$]$_2$** (▲) in MeCN at 298 K.

Table 2. Photophysical[a] and electrochemical[b] data for the compounds in this work.

Compound	**1Br$_2$**	**1[PF$_6$]$_2$**	**2[PF$_6$]**	**3[PF$_6$]$_2$**	**5[PF$_6$]$_2$**	**6[PF$_6$]$_2$**
λ_{max} [nm]	303 (3.27)	303 (3.34)	291 (13.2)	275 (5.11)	284 (23.0)	297 (12.7)
(ε_{max} [10^3 $M^{-1}cm^{-1}$])	315 (3.47)	315 (3.34)	299 (13.2)	315 (4.16)	313 (9.62)	348 (11.8)
	329 sh	329 sh	312 sh	331 sh	329 sh	439 (12.3)
	384 sh	387 sh	326 sh	395 sh	439 sh	
	406 (16.4)	406 (21.5)	415 (0.69)	415 (23.4)	464 (27.3)	
λ_{em} [nm]	467	469	476	481	545	599
Φ_{PL} [%]	33	42	29	22	60	0.2
τ_e [ns]	3.84	3.99	3.98	4.25	6.78	6.60
$E^1_{½}$ [V] (ΔEp [mV])	−0.61 (112)	−0.61 (101)	−1.26[c]	−0.74[c]	−0.22[c]	−0.59[c]
$E^2_{½}$ [V] (ΔEp [mV])	−1.22 (82)	−1.26 (79)		−1.22 (60)	−0.80[c]	−1.09[c]

[a]In deaerated acetonitrile at 298 K. Quinine sulfate was used as the reference (Φ_{PL} = 54.6% in 0.5 M H_2SO_4 at 298 K)[22] in all cases except for **6[PF$_6$]$_2$**, for which [Ru(bpy)$_3$][PF$_6$]$_2$ was used (Φ_{PL} = 9.5% in deaerated acetonitrile at 298 K).[23] [b]Measurements were performed at 100 mV s^{-1} in deaerated MeCN solution at 298 K using Fc/Fc$^+$ as an internal standard, and are referenced with respect to SCE (Fc/Fc$^+$ = 0.38 V in MeCN). [c]Irreversible process, Ep$_c$ value quoted.

As might be expected, changing the counterion from **1Br$_2$** to **1[PF$_6$]$_2$** causes very little change in the absorption spectra. At high energies, there are multiple bands or shoulders (303, 315 and 329 nm), which demonstrate virtually identical absorptivities regardless of the counter ion. Similarly, at lower energies (384-387 and 406 nm) the form of the spectra is unchanged, although the absorptivity observed for **1Br$_2$** in this part of the spectrum is slightly lower than for **1[PF$_6$]$_2$**. The methyl substituents in **3[PF$_6$]$_2$** do not appreciably alter the spectra compared to **1[PF$_6$]$_2$**, with only the CT band undergoing a small 534 cm^{-1} red-shift with a moderate increase in absorptivity. This red-shift, invoked by the electron-donating nature of the methyl groups, points to localisation of the HOMO on regions of the molecule adjacent to the charged nitrogen atoms. This is supported by the greater red-shift of the CT band (1851 cm^{-1} compared to **1[PF$_6$]$_2$**) induced by the more electron-donating 2-thienyl groups of **6[PF$_6$]$_2$**. The extended aromaticity in **5[PF$_6$]$_2$** pushes the CT band even more to the red, by 3079 cm^{-1} compared to **1[PF$_6$]$_2$**.

While the CT bands vary significantly based on the aromaticity and substituents of the dihydrohelicenes, the high energy bands are largely unaffected. The only noticeable changes come with **5[PF$_6$]$_2$**, whose extended aromaticity increases the overall absorptivity, and with **6[PF$_6$]$_2$** which demonstrates an additional π-π* transition at 348 nm associated with the 2-thienyl units.

The ring-opened intermediate **2[PF$_6$]** has no enforced coplanarity of the pyridyl and imidazolyl rings. As a result, the only pronounced bands are the high energy π–π* transitions, localized on the individual pyridyl and imidazolyl rings, which show reasonably large absorptivities in the region of ~13000 $M^{-1}cm^{-1}$; by comparison, the low energy pyridyl-imidazolyl CT transition is poorly absorbing (<700 M^{-1} cm^{-1}) since there is poor orbital overlap between the two mutually orthogonal heterocycles. Upon ring closure to generate **3[PF$_6$]$_2$**, the absorptivity drastically increases, indicating significantly improved orbital overlap facilitating the CT transition.

Compounds **1Br$_2$**, **1[PF$_6$]$_2$**, **2[PF$_6$]** and **3[PF$_6$]$_2$** are deep blue emitters, while **5[PF$_6$]$_2$** and **6[PF$_6$]$_2$** are green-yellow and orange in color, respectively (Table 2, Fig. 3). The emission spectra of **1Br$_2$** and **1[PF$_6$]$_2$** overlap, indicating that the counterion plays no role in the emission process. The methyl groups in **3[PF$_6$]$_2$** induce a small 532 cm^{-1} red-shift in λ_{em} compared to **1[PF$_6$]$_2$**, supporting the assertion that they are primarily modulating the electronics of the HOMO; a very large red-shift of 4629 cm^{-1} observed for **6[PF$_6$]$_2$**, bearing electron donating 2-thienyl substituents, is also consistent with this assignment. Extending the aromaticity in **5[PF$_6$]$_2$** also red-shifts emission. Interestingly, despite its only bearing one charged center, **2[PF$_6$]** demonstrates similar photophysical properties to **3[PF$_6$]$_2$**, with a blue-shift of only 218 cm^{-1}. All the compounds show emission lifetimes in the nanosecond regime, which indicate fluorescence. Compounds **1Br$_2$**, **1[PF$_6$]$_2$**, **2[PF$_6$]** and **3[PF$_6$]** are the shortest, in the range of 3.84-4.25 ns, while **5[PF$_6$]$_2$** and **6[PF$_6$]** are 6.60-6.78 ns.

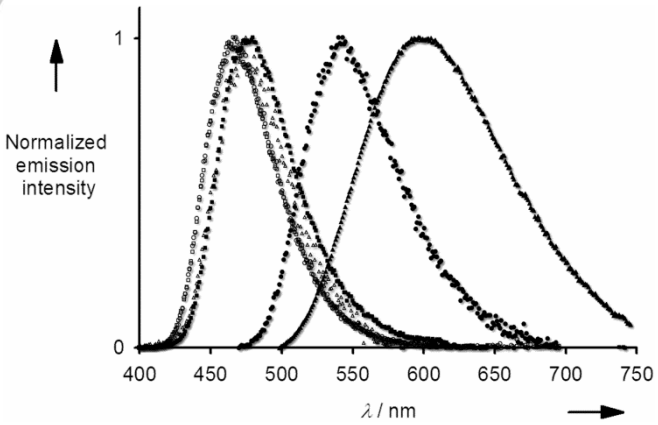

Figure 3. Normalized emission spectra of **1Br$_2$** (□), **1[PF$_6$]$_2$** (○), **2[PF$_6$]** (△), **3[PF$_6$]$_2$** (■), **5[PF$_6$]$_2$** (●) and **6[PF$_6$]$_2$** (▲) in deaerated MeCN at 298 K.

Although a number of emissive helical cationic-type molecules have been reported,[8,10,21] their Φ_{PL} values were not usually determined which makes comparisons difficult. However,

Clennan and co-workers recently reported a dicationic helicene, which contained two *N*-methylated quarternary ammonium centers, that emitted with Φ_{PL} = 6.6 %.[10] In contrast, the compounds in this work, whose quarternary N atom is contained within an aliphatic heterocycle, are much brighter with Φ_{PL} as high as 60% in the case of **5[PF$_6$]$_2$**. Here the brightness of the emission is enhanced through rigidification of the dihydrohelicene framework by the quinolinyl units. Only **6[PF$_6$]$_2$** was found to be poorly emissive, which we ascribe to a "loose bolt" effect resulting from the large 2-thienyl units.

Finally, the relevant electrochemical data are summarized in Table 2.[17] All compounds except for **2[PF$_6$]** show two *quasi*-reversible or irreversible one-electron reduction steps, as has been frequently observed for other dicationic heliquats.[9,10] **2**[**PF$_6$**] only shows a single poorly resolved reduction wave. No oxidation waves were observed except in the case of **1Br$_2$**, which was attributed to oxidation of bromide.

The reduction waves of **1Br$_2$** and **1[PF$_6$]$_2$** are virtually identical, as expected. Surprisingly, in spite of the small red-shift in absorption and emission observed for **3[PF$_6$]$_2$**, the first reduction wave is 0.11 V lower than **1[PF$_6$]$_2$**. The E_{pc} values mirror this, with the value appearing at −0.57 V for **1Br$_2$** and **1[PF$_6$]$_2$**, but at −0.65 V for **3[PF$_6$]$_2$**. However, the second wave is largely unchanged. **5[PF$_6$]$_2$**, by virtue of its extended aromaticity, sees a large anodic shift in both reduction waves. In comparison, **6[PF$_6$]$_2$** undergoes a more modest change, consistent with the suggestion that the 2-thienyl groups are largely modulating the electronics of the HOMO. Interestingly, the reduction potential for **2[PF$_6$]** largely matches those of **1Br$_2$**, **1[PF$_6$]$_2$** and **3[PF$_6$]$_2$**. This suggests that the second reduction process observed for the dicationic species is attributable to reduction of the imidazolium moiety, and thus the first wave – which is not observed for **2[PF$_6$]** – can be ascribed to reduction of the pyridinium moiety.

In conclusion, a one-pot synthesis of a family of helical dications has been reported. Solutions of **1[PF$_6$]$_2$-5[PF$_6$]$_2$** are highly fluorescent, with emissions ranging from the blue to orange. The emission from **6[PF$_6$]$_2$** was significantly weaker, which was ascribed to increased non-radiative decay due to the "loose bolt" effect of the pendant 2-thienyl units.

Experimental Section

Synthetic procedures and characterization data for all the compounds in this work, as well as details of the instrumentation and procedures used for the spectroscopic and electrochemical measurements and the crystal structure determinations, are given in the Supporting Information.[17]

Acknowledgements

This work was funded by the EPSRC (EP/I014039/1). Biological testing was performed at the Institute of Cancer Therapeutics, University of Bradford, UK. EZ-C acknowledges the University of St Andrews for funding and Prof. Ifor D.W. Samuel for access to the emission spectrometer. CT thanks MUSA for financial support.

Keywords: Helical compounds • fluorescence • crystal structure • voltammetry • cytotoxicity

[1] Y. Shen, C.-F. Chen, *Chem. Rev.* **2012**, *112*, 1463–1535.
[2] a) M. Gingras, *Chem. Soc. Rev.* **2013**, *42*, 968–1006; b) M. Gingras, G. Félix, R. Peresutti, *Chem. Soc. Rev.* **2013**, *42*, 1007–1050.
[3] M. Gingras, *Chem. Soc. Rev.* **2013**, *42*, 1051–1095.
[4] A. Urbano, M. C. Carreno, *Org. Biomol. Chem.* **2013**, *11*, 699–708.
[5] Z. Peng, N. Takenaka, *Chem. Record* **2013**, *13*, 28–42.
[6] R. Amemiya, M. Yamaguchi, *Org. Biomol. Chem.* **2008**, *6*, 26–35.
[7] K. Watanabe, K. Suda, K. Akagi, *J. Mater. Chem. C* **2013**, *1*, 2797–2805.
[8] L. Adriaenssens, L. Severa, T. Šálová, I. Císařová, R. Pohl, D. Šaman, S. V. Rocha, N. S. Finney, L. Pospíšil, P. Slavíček, F. Teplý, *Chem. Eur. J.* **2009**, *15*, 1072–1076.
[9] L. Pospíšil, L. Bednárová, P. Štěpánek, P. Slavíček, J. Vávra, M. Hromadová, H. Dlouhá, J. Tarábek, F. Teplý, *J. Am. Chem. Soc.* **2014**, *136*, 10826–10829.
[10] X. Zhang, E. L. Clennan, N. Arulsamy, *Org. Lett.* **2014**, *16*, 4610–4613.
[11] a) A. Rajca, S. Rajca, M. Pink, M. Miyasaka, *Synlett* **2007**, 1799–1822; b) T. Biet, A. Fihey, T. Cauchy, N. Vanthuyne, C. Roussel, J. Crassous, N. Avarvari, *Chem. Eur. J.* **2013**, *19*, 13160–13167.
[12] a) L. Norel, M. Rudolph, N. Vanthuyne, J. A. G. Williams, C. Lescop, C. Roussel, J. Autschbach, J. Crassous, R. Reau, *Angew. Chem.* **2010**, *122*, 103–106; *Angew. Chem. Int. Ed.* **2010**, *49*, 99–102; b) E. Anger, M. Srebro, N. Vanthuyne, L. Toupet, S. Rigaut, C. Roussel, J. Autschbach, J. Crassous, R. Reau, *J. Am. Chem. Soc.* **2012**, *134*, 15628–15631.
[13] a) L. Shi, Z. Liu, G. Dong, L. Duan, Y. Qiu, J. Jia, W. Guo, D. Zhao, D. Cui, X. Tao, *Chem. Eur. J.* **2012**, *18*, 8092–8099; b) J.-Y. Hu, A. Paudel, N. Seto, X. Feng, M. Era, T. Matsumoto, J. Tanaka, M. R. J. Elsegood, C. Redshaw, T. Yamato, *Org. Biomol. Chem.* **2013**, *11*, 2186–2197.
[14] E. C. Campbell, E. E. Glover, G. Trenholm, *J. Chem. Soc. C* **1969**, 1987–1990.
[15] Glover et al. proposed a mechanism of formation of **1Br$_2$** involving the coupling of two molecules of (2-bromoethyl)pyridin-2-ylmethylene-imine initiated by intermolecular nucleophilic attack of a pyridyl N atom at a bromoethyl group.[14] Our isolation of **2[PF$_6$]** and **4[PF$_6$]** contradicts that scheme, by implying that closure of the dihydropyrazinium ring is the final step of the transformation. An alternative mechanistic sequence accounting for this observation is drawn in the Supporting Information.[17]
[16] L. J. Kershaw Cook, R. Mohammed, G. Sherborne, T. D. Roberts, S. Alvarez, M. A. Halcrow, *Coord. Chem. Rev.*, doi: 10.1016/j.ccr.2014.08.006.
[17] Additional Tables and Figures for the crystal structures and voltammograms; NMR, NOESY and photophysical data; a proposed mechanism for the synthesis of **1^{2+}**; and all experimental details are given in the Supporting Information.
[18] This H…H distance is only approximate, since the H atoms in the crystal structure were placed in calculated positions during the structure refinement.
[19] a) M. J. Hannon, *Chem. Soc. Rev.* **2007**, *36*, 280–295; b) B. M. Zeglis, V. C. Pierre, J. K. Barton, *Chem. Commun.* **2007**, 4565–4579; c) H.-K. Liu, P. J. Sadler, *Acc. Chem. Res.* **2011**, *44*, 349–359.
[20] a) H. Ihmels, D. Otto, *Top. Curr. Chem.* **2005**, *258*, 161–204; b) A. Rescifina, C. Zagni, M. G. Varrica, V. Pistarà, A. Corsaro, *Eur. J. Med. Chem.* **2014**, *74*, 95–115.
[21] M. Čížková, D. Šaman, D. Koval, V. Kašička, B. Klepetářová, I. Císařová, F. Teplý, *Eur. J. Org. Chem.* **2014**, 5681–5685.
[22] W. H. Melhuish, *J. Phys. Chem.* **1961**, *65*, 229–235.
[23] H. Ishida, S. Tobita, Y. Hasegawa, R. Katoh, K. Nozaki, *Coord. Chem. Rev.* **2010**, *254*, 2449–2458.

Entry for the Table of Contents

COMMUNICATION

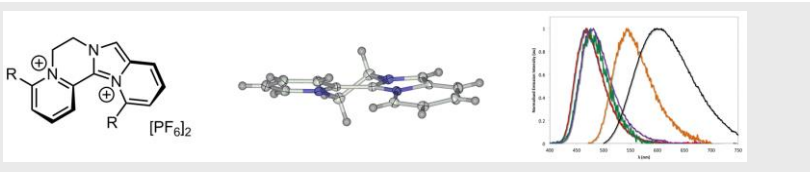

A. Santoro, R. M. Lord, J. J. Loughrey, P. C. McGowan, M. A. Halcrow*, A. F. Henwood, C. Thomson, E. Zysman-Colman**

Page No. – Page No.

One-Pot Synthesis of Highly Emissive Dipyridinium Dihydrohelicenes

Condensation of a pyridyl-2-carbaldehyde derivative with 2-(bromoethyl)amine hydrobromide affords tetracyclic pyrido[1,2-*a*]pyrido[1',2':3,4]imidazo-[2,1-*c*]-6,7-dihydropyrazinium dications in excellent yields. These afford unusually bright emissions for helicene-like compounds, with Φ_{PL} as high as 59.9% in the range of 460-600 nm. Preliminary cytotoxicity studies against the HT-29 cancer cell line demonstrated moderate-to-good activity, with IC_{50} values 12-30x that of cisplatin.